A New Approach to Improve PV Power Injection in LV Electrical Systems using DVR

Hossein Sagha, Ghassem Mokhtari, Ali Arefi, *Senior Member, IEEE*, Ghavameddin Nourbakhsh, *Member, IEEE*, Gerard Ledwich, *Senior Member, IEEE* and Arindam Ghosh, *Fellow, IEEE*

***Abstract*— With increasing photovoltaic (PV) penetration in low voltage (LV) distribution networks, voltage violation during the peak PV generation period is one of the main power quality concerns. To minimize the PV power curtailment caused by voltage violations, this paper proposes a new approach utilizing one dynamic voltage restorer (DVR) at the secondary of existing urban distribution transformer as a continuous voltage compensator with an accompanying control algorithm. The voltage compensation algorithm controls the DVR in real-time to prevent over-voltage and under-voltage at all network nodes, thereby maximizing PV injection and preventing equipment damage. The controller uses the equivalent line impedance of network to estimate the average voltage of load points without the need for any communication links for measuring load voltages. In this approach, the fixed tap changer of the distribution transformer is also optimally adjusted to minimize the DVR rating using a proposed offline optimization method. Simulation results on IEEE LV test feeder prove the ability of the DVR in maintaining all network node voltages within the allowable range in peak demand and peak PV generation periods with the benefit of injecting only a small amount of active and reactive power to the system, in contrast to alternative algorithms.**

***Index Terms*—Communication-less control, Dynamic voltage restorer, Low voltage distribution network, Optimal tap setting, Photovoltaic penetration, Power quality, Voltage regulation**

I. Introduction

TRADITIONALLY, low voltage (LV) grids are designed to operate satisfactorily especially during peak demand periods to avoid high voltage drops and to keep voltage magnitudes within standard limits across the network. Thus, in order to prevent unacceptable under-voltage, the distribution transformer tap changer is usually set in the range of +2% to +5%. However, in recent years the photovoltaic (PV) uptake has been increasing with the growth of 60% per annum [1]. Therefore, with this range of tap settings, high local PV power injections that normally coincide with low demand periods cause increasing incidence of over-voltage in the network based on current standards, as reported in [2-4]. For example, the Australian standard 'AS 61000.3.100: steady state voltage limits in public electricity systems' defines the allowable range of +6% to -6% for 240 V and a preferred range of +6% to -2% for 230 V nominal voltage [5]. In addition to these violations, over-voltage brings safety and protection issues as well as the likelihood of damaging equipment or reducing its lifetime [6]. This is an ongoing problem that becomes more probable as PV penetration in Australian distribution networks increases [7-9]. IEEE standard for grid-connected PVs suggests that PV inverter should be disconnected if its terminal voltage passes an upper limit [10]. This practice increases the amount of curtailed renewable energy due to over-voltage incidents, resulting in a reduction of PV penetration and related benefits.

Some approaches are investigated in literature to solve this problem associated with PVs. One approach is the on-load tap changer (OLTC) in which an appropriate secondary voltage level is maintained by stepping between multiple tap settings automatically [11, 12]. The main disadvantages of this approach are limited voltage taps, discrete operation, intentional time delay to prevent unnecessary tap changes during transient voltage fluctuations and inability to mitigate three-phase unbalance. Another method is the local active power curtailment (APC) which is used to reduce the voltage rise and prevent PV inverters from tripping [3, 13]. The drawback of this strategy is curtailed renewable energy generation unless storage devices are utilized to store the excess PV energy, which introduces high investment costs [14, 15]. Single-point or distributed reactive power (Q) injection is also performed for voltage compensation using devices such as static VAR compensators (SVC) and distribution static synchronous compensator (D-STATCOM). The latter one has the advantage of fast response time and consequently, providing dynamic voltage control in distribution systems [16]. It is important to note that generally single-point voltage compensation is less effective than distributed compensation [17]. Nonetheless, the cost of distributed compensators, which may require coordination for more effective compensation during various system conditions, is high [18, 19]. Another similar method is power factor control (PFC) in which Q is injected through distributed generation (DG) units [20-23]. Nevertheless, for Q injection, DG units require a higher VA capacity or the amount of their active power (P) injection may

This work was supported in part by the Australian Research Council (ARC) under ARC Discovery Grant DP110104554.

H. Sagha is with EDMI Ltd Smart Energy Solutions, Brisbane, Australia (e-mail: hosseins@edmi.com.au).

G. Mokhtari is with the Australian e-Health Research Centre, CSIRO, Brisbane, Australia (e-mail: ghassem.mokhtari@csiro.au).

A. Arefi is with School of Engineering and Information Technology, Murdoch University, Perth, Australia (email: a.arefi@murdoch.edu.au)

G. Nourbakhsh and G. Ledwich are with the School of Electrical Engineering and Computer Science, Queensland University of Technology, Australia (e-mails: g.nourbakhsh@qut.edu.au; g.ledwich@qut.edu.au).

A. Ghosh is with the Department of Electrical and Computer Engineering, Curtin University, Perth, Australia (e-mail: arindam.ghosh@curtin.edu.au).

need limiting. Q injection, however, increases losses, reduces network P capacity and is not very effective in voltage regulation because the X/R ratio of line impedances in LV grids is not high [24]. Finally, trying to solve the problem at the consumer side using automatic voltage regulators at individual load points is not a cost effective solution.

For implementing the aforementioned approaches, various methods are proposed which can generally be categorized as follows: 1) Centralized methods that require a wide and costly range of communication links and extensive systems for coordinating different devices in the network. Smart inverters are mainly rely on this type of information exchange [3, 20-22]; 2) Semi-coordinated [12] and 3) Decentralized methods that require reduced or no communication links to control DG units locally while coordinating every unit with no or a limited number of network devices [14, 25]. The latter methods have the benefit of faster response to local voltage variations [16]. However, it is neither economical nor technically favorable to use methods that mainly rely on communication links because of their vulnerability to interruptions that compromises algorithm reliability.

With reference to the shortcomings noted in the literature review, this paper proposes the utilization of a dynamic voltage restorer (DVR) to manage voltage issues in LV distribution systems without a centralized or semi-coordinated controller. DVR is a series compensator which is mainly placed at sensitive loads to regulate the voltage tightly and rapidly [26, 27]. Compared to SVC, D-STATCOM and PFC, it requires much lower device rating for the same level of voltage regulation. Moreover, the flexibility and effectiveness of the DVR and the recent advances in its design including storage-less ac-ac converter [28], double dc link [29], fault current-limiting [30], integrated DVR-ultra capacitor [31] and transformer-less [32] designs make it more cost-effective and justifiable for application in LV distribution systems. The proposed compensation approach in this paper can be applied to existing distribution systems for real-time voltage compensation using local information only. This local control approach can prevent both over-voltage and under-voltage and their associated issues including PV power curtailment.

Therefore, the main contribution of this paper includes:

- A new approach using DVR series voltage compensation at the secondary of a distribution transformer to deal with over- and under-voltage at all nodes in a LV network. This approach offers a state of the art technology with online and continuous voltage regulation without the need for communication links, which is currently not available in LV networks. This is achieved by injecting only small amounts of P and Q to the system in contrast to present methods.
- A new real-time algorithm for estimating average deviation of downstream node voltages for the compensation purpose.
- A new optimum fixed tap setting for distribution transformer with minimal DVR rating requirement, through an efficient offline optimization approach that uses only two extreme load levels obtained from annual profile data.

The paper is organized as follows. Section II illustrates the proposed system configuration and control algorithm. The optimal tap adjustment and load flow analysis are discussed in Sections III and IV, respectively. Simulation results, followed by relevant conclusions are presented in Sections V and VI.

II. Continuous Voltage Compensation Algorithm

In the proposed application, the DVR is connected in series with the network at the secondary of the distribution transformer. It pulls the voltage up or down at its downstream side, thereby compensating load voltages. Since load voltage profiles in an LV network usually have a good positive correlation at each time window, the proposed algorithm maintains load voltages within the permissible range as discussed in Section V. The converter structure can either include an injection transformer or be transformer-less. The isolation transformer provides galvanic isolation and simplifies the converter topology to have one DC-link as well as making protection equipment less complex [33]. As discussed in Section V, the low output voltage level of DVR reduces the cost and volume of this low-frequency injection transformer. In the same section, it is illustrated that the converter needs a low rating and low cost power supply and storage unit for P injection requirement of the algorithm. Moreover, the protection of DVR in an LV network is simpler due to the very low short-circuit level at the LV side. Usually, DVRs are equipped with a shunt breaker for bypassing the DVR once a fault condition is detected [33].

Since LV grids are usually unbalanced and have different phase characteristics, the algorithm is developed and applied per phase. The control system of the DVR measures some local electrical data including bus voltage at the DVR upstream side as well as the DVR branch current as depicted in Fig. 1. In this figure, the distribution network is replaced with an equivalent circuit and T is the setting of the tap changer. V_e is the network equivalent voltage that is the estimation of the average of load point voltages all over the network by the proposed method. The aim of the proposed control algorithm is to regulate the magnitude of V_e to the pre-specified value of 1 per unit (pu) in order to minimize bus voltage deviations in all three phases and all loading conditions of the network over the entire year.

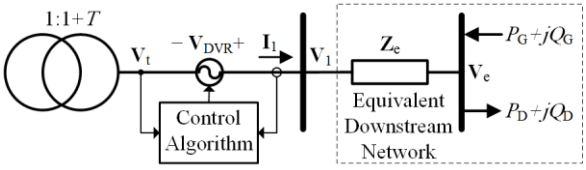

Fig. 1. Per-phase plot of proposed structure for LV grid voltage regulation.

Since demand and generation vary with time, the proposed algorithm estimates the deviation of V_e in real-time, based on which, the DVR voltage is adjusted continuously to regulate downstream bus voltages. The local information available for DVR controller are the DVR phasor current $\mathbf{I}_1$ and the transformer secondary phasor voltage $\mathbf{V}_t$ with the magnitude equal to $1+T$ pu. Therefore, $\mathbf{V}_e$ can be estimated as:

$$\mathbf{V}_e^j = \mathbf{V}_t^j + \mathbf{V}_{DVR}^j - \mathbf{Z}_e^j \mathbf{I}_1^j, \quad (1)$$

where $\mathbf{V}_{\text{DVR}}$ is the DVR phasor voltage and $j \in \{\text{a},\text{b},\text{c}\}$ indicates the three phases. $\mathbf{Z}_{\text{e}}$ is the equivalent line impedance for the downstream network, which is obtained offline. Various methods are proposed in literature for calculating $\mathbf{Z}_{\text{e}}$ which are either very analytical [34] or based on the maximum voltage not the average voltage of load points [35]. For the aim of regulating average voltage deviation, an averaging method for estimating this impedance is developed as given in (2) which uses the results of the load flow analysis considering a uniform loading at all load points. As shown in Section V, since this value represents the equivalent impedance of the network seen from DVR point, our estimation is also accurate for general non-uniform loads in a distribution network.

$$\mathbf{Z}_{\text{e}}^{j} = \sum_{i \in B^{j}} \left(\mathbf{V}_{1}^{j} - \mathbf{V}_{i}^{j} \right) \Big/ N^{j} \mathbf{I}_{1}^{j}, \tag{2}$$

where N is the number of load points, B includes load point bus numbers, and $\mathbf{V}_1$ and $\mathbf{V}_i$ are the first and i-th bus phasor voltage, respectively. The phase unbalance of the three-phase system is also improved when the proposed control algorithm regulates the equivalent phase angles to the reference three-phase angles. Thus, in order to regulate the average voltage magnitude to the pre-specified value of V_{ref} and regulate the phase angle to that of $\mathbf{V}_{\text{t}}$, DVR voltage is calculated based on the obtained $\mathbf{Z}_{\text{e}}$ and the locally measured parameters using (1) as given in (3) and demonstrated in Fig. 2.

$$V_{\text{DVR}}^{j} \angle \phi_{V_{\text{DVR}}}^{j} = (V_{\text{ref}} - V_{\text{t}}) \angle \phi_{V_{\text{t}}}^{j} + Z_{\text{e}}^{j} I_{1}^{j} \angle \left(\phi_{Z_{\text{e}}}^{j} + \phi_{I_1}^{j} \right), \tag{3}$$

where the reference phase angle can be considered as that of $\mathbf{V}_{\text{t}}$ on each phase, and thus, $\phi_{V_{\text{t}}}$ is zero for all phases.

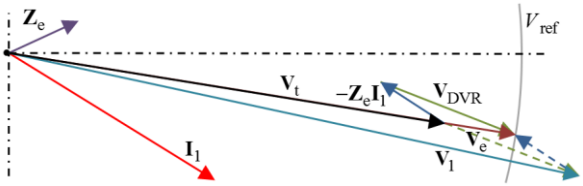

Fig. 2. Phasor diagram for compensation of the network equivalent voltage.

This reference voltage is followed by the DVR switching inverter output, which is controlled by a closed loop algorithm. The details of designing the inverter control algorithm does not fit in the scope of this paper and is described in depth in [36] along with implementation results using Typhoon HIL 400.

III. Optimized Tap Setting

In general, many factors can affect the required DVR rating for an effective compensation, of which location and use of multiple DVRs, however costly, are the decisive factors. For long rural feeders, evaluating the optimal location of the DVR is important [37]. However, most urban distribution feeders are not very long; thereby a single DVR is sufficient for their voltage regulation. In addition, optimal location(s) of single or multiple DVRs would not guarantee to retain optimality in the future, and therefore, it asks for extensive long-term forecasting and planning outside the scope of this paper, as described in [38]. However, DVR placement at the transformer substation site may not be optimal, but from operation and economic point of view, it is a very good candidate.

Amongst other factors, rating mainly depends on the peak PV generation and peak demand levels in which the highest voltage deviations and network currents are encountered. In addition, the tap setting has a considerable effect on the required DVR rating [39]. For instance, an electrical system with higher voltage rises compared to voltage drops can be regulated with less DVR effort when the tap is set to less than unity. Since voltage drops are also reduced by DVR compensation, the probability of under-voltage will be reduced in this case even with this lower tap setting. Therefore, in order to find the minimum required nominal DVR rating along with the optimal tap setting, an offline optimization method is utilized. Through the offline optimization, a load flow analysis as described in Section IV is performed to find the load point voltages and branch currents. For reducing the computation time of the optimization process, two load levels obtained from yearly load profiles of the network are considered. One load level represents the network at the time with maximum PV generation during the year called *G*, and another load level represents the network at the time with maximum demand during that year called *D*. Thus, the computational effort of optimization process is reduced to only two load flow analyses in the optimization iterations instead of evaluating numerous load levels for a whole year.

In the proposed approach, distribution transformers are not equipped with on-line tap changer. Thus, adjusting the tap setting is implemented only once per year. Actually, tap setting does not need any further adjustments until network loads are significantly changed in future. Therefore, the optimal tap setting is valid for at least a year until new data is collected from the network for another year. This also implies considering a margin for the obtained DVR rating taking into account the load growth.

The decision variables are represented with a solution vector in a thirteen-dimensional optimization hyperspace, twelve of which are real values equal to the DVR voltage magnitude and phase angle at two load levels l for each phase j, $x_V^{j,l} = V_{\text{DVR}}^{j,l}$ and $x_\phi^{j,l} = \phi_{V_{\text{DVR}}}^{j,l}$ with $l \in \{G, D\}$ and $j \in \{\text{a},\text{b},\text{c}\}$, and the last variable is a discrete value equal to the tap setting of distribution transformer, X_{tap}=T. The optimization finds optimum values for these decision variables in order to minimize the cost function as illustrated in (4).

$$\begin{aligned} &\left\{ x_V^{j,l}, x_\phi^{j,l}, X_{\text{tap}} \right\} = \arg\min(J), \\ &\text{Subject to: } V_{\text{lo}} \le V_i^{j,l} \le V_{\text{hi}},\ i \in B^{j},\ j \in \{\text{a},\text{b},\text{c}\},\ l \in \{G, D\}, \end{aligned} \tag{4}$$

where V_{lo} and V_{hi} are the standard lower and upper voltage limits, $V_i^{j,l}$ is the voltage magnitude of i-th bus of j-th phase at the l-th load level. The cost function J is defined as the sum of maximum three-phase DVR output power and voltage

unbalance factor deviation (VUFD), as given in (5).

$$J = 3\left[\max\left(I_1^{j,l}\right)\max\left(V_{\mathrm{DVR}}^{j,l}\right)\right] + w\max(\mathrm{VUFD}^{l}) + p\left(V_i^{j,l}\right) \quad (5)$$

$I_1^{j,l}$ is the DVR current magnitude at *l*-th load level of *j*-th phase, *w* is the optimization weighting factor, and *p* is the penalty function. In each iteration, load flow analysis at both load levels is performed to calculate the cost function. Voltage limit constraints are also checked, and if a violation occurs in any load point and at any load level, the cost function is penalized with a high cost value multiplied by the number of voltage violations in order to find a solution with minimum voltage violations possible. The VUFD is calculated based on the load flow results as follows using symmetrical bus voltage components V^{12} [40]:

$$\mathrm{VUFD} = \sqrt{\left(\sum_j \sum_{i\in B^j} \left|V_i^2 / V_i^1\right|^2\right) \Big/ \sum_j N^j} \times 100\% \quad (6)$$

For solving (4), simulated annealing (SA) and particle swarm optimization (PSO) [41] approaches are compared in Section V. SA has the benefit of not requiring a particle population, being easier to code and having a higher probability of avoiding local optima and converging to the global optimum solution, as the number of iterations are increased [42]. However, it has longer convergence time compared to PSO, and for avoiding local optima, PSO is combined with genetic algorithm (GA) crossover and mutation techniques. The whole design process can be summarized as illustrated in the flow chart of Fig. 3.

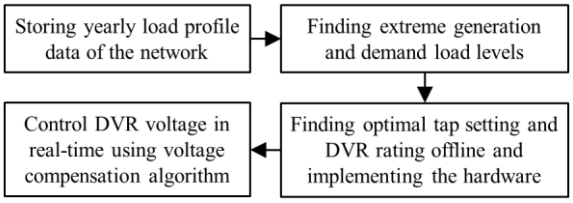

Fig. 3. Flow chart of the system design process.

IV. Load Flow Analysis

The direct load flow (DLF) analysis [43], which is a very fast method, is used to reduce the convergence time of the iterative optimization process and decrease the simulation time. In this analysis, the calculation of voltage deviations is modified by adding the effect of the DVR voltage on downstream buses as given in (7).

$$\mathbf{V}_1^{\mathrm{abc}} = \mathbf{V}_{\mathrm{t}}^{\mathrm{abc}} + \mathbf{V}_{\mathrm{DVR}}^{\mathrm{abc}} \quad (7)$$

The load flow algorithm is also modified for analyzing unbalanced three-phase systems. Zero, positive and negative sequence of bus current injections, namely matrix $\mathbf{I}^{012} = [\mathbf{I}^0\ \mathbf{I}^1\ \mathbf{I}^2]^{\mathrm{T}}$, are calculated using three-phase phasors of bus current injections, namely matrix $\mathbf{I}^{\mathrm{abc}}=[\mathbf{I}^{\mathrm{a}}\ \mathbf{I}^{\mathrm{b}}\ \mathbf{I}^{\mathrm{c}}]^{\mathrm{T}}$, to find the symmetrical voltage drops, namely $\Delta\mathbf{V}^{012}$, and consequently, three-phase bus voltages $\mathbf{V}^{\mathrm{abc}}$ as given in the followings.

$$\begin{aligned}
&\left[\mathbf{I}^{\mathrm{abc}}\right] = \left[\left(\mathbf{S}^{\mathrm{abc}} \oslash \mathbf{V}^{\mathrm{abc}}\right)^*\right],\\
&\left[\mathbf{I}^{012}\right] = \mathbf{A}^{-1}\left[\mathbf{I}^{\mathrm{abc}}\right],\\
&\left[\Delta\mathbf{V}^{012}\right] = \left[\mathbf{DLF}^{012}\right]\left[\mathbf{I}^{012}\right],\\
&\left[\mathbf{V}^{\mathrm{abc}}\right] = \left[\mathbf{V}_{\mathrm{t}}^{\mathrm{abc}}\right] + \left[\mathbf{V}_{\mathrm{DVR}}^{\mathrm{abc}}\right] - \mathbf{A}\left[\Delta\mathbf{V}^{012}\right],
\end{aligned} \quad (8)$$

where $\mathbf{S}^{\mathrm{abc}}$ is the bus apparent power injection, $\oslash$ is element-wise division, and $[\mathbf{DLF}^{012}]$ is defined as given in (9).

$$\left[\mathbf{DLF}^{012}\right] = \begin{bmatrix}\left[\mathbf{DLF}^{0}\right] & 0\\ 0 & \mathbf{I}_{2\times 2}\otimes\left[\mathbf{DLF}\right]\end{bmatrix}, \quad (9)$$

where $[\mathbf{DLF}]$ is the positive sequence and $[\mathbf{DLF}^0]$ is the zero sequence of DLF matrix obtained using zero sequence line impedances for considering the neutral impedance, $\otimes$ is the tensor product, and

$$\mathbf{A} = \begin{bmatrix}1 & 1 & 1\\ 1 & \alpha^2 & \alpha\\ 1 & \alpha & \alpha^2\end{bmatrix}\otimes\mathbf{I}, \quad \alpha = e^{j\frac{2}{3}\pi}, \quad (10)$$

where $\mathbf{I}$ is the identity matrix with dimensions equal to the number of branches in each phase.

V. Simulation Studies

The Three-phase non-uniform IEEE European LV test feeder [44], depicted in Fig. 4, is modeled in MATLAB. It is used for evaluating the proposed optimization and voltage compensation algorithms and comparing with alternative methods. In this case, the daily load profiles are increased by 25% to indicate the worst case at peak demand during a year and to account for load growth in future. The test feeder data did not include PV power injection profiles. Therefore, in this study, all load points are assumed to have PV injection capacity equal to the peak demand of that point in order to simulate a future electrical system with high PV penetration. The daily PV power profiles were extracted from year 2012-2013 solar home electricity data [45] in a summer day with highest PV injection in order to obtain the worst case of the PV generation during a year. The design of PV inverter control algorithm as described in [46] is out of the scope of this paper, and therefore, they are modelled as simple PQ injection nodes.

IEEE test feeder consists of a 0.8 MVA Δ-Y connected distribution transformer with the voltage ratio of 11/0.416 kV and constant power loads with a power factor of 0.95. The standard limits for voltage magnitude variations are +6% to -6%. The key system parameters including total peak demand and total peak PV generation as well as the number of load points at each phase are given in Table I. To demonstrate the worst cases, the peak values correspond to the maximum demand with zero PV injection and the maximum PV generation with zero demand during the aforementioned high demand and high PV generation periods, respectively. These two peak levels are considered as the two load levels of *l* for

optimizing DVR size and tap setting. The values for these two levels also show that the total peak demand is about one-third to half of the total peak PV generation because peak PV power injections are more coincidental than peak load demands. The equivalent line resistance and reactance calculated using (2) for this test network for each phase are also reported in Table I.

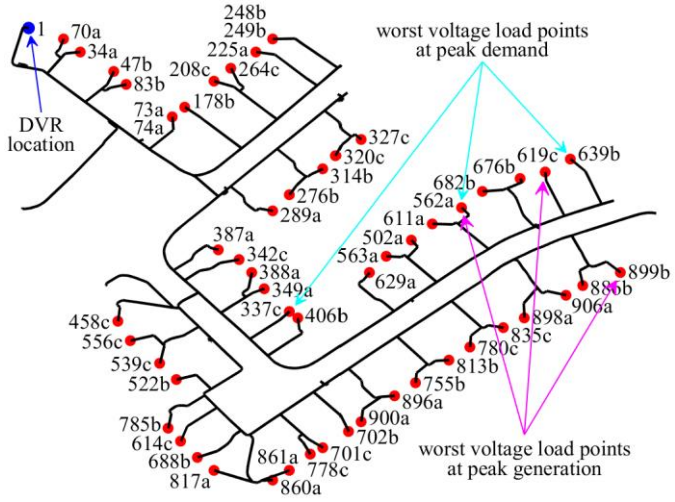

Fig. 4. Three-phase European LV test feeder with load points and their corresponding bus number and phase. Load points with the worst voltage deviation are also indicated by arrows.

TABLE I
Key parameters of three-phase LV test system

Phase	**a**	**b**	**C**	**feeder**
Peak demand P (kW)	30.0	48.4	25.7	104
Peak PV generation (kW)	103	94.5	80.8	278
Number of load points (N^j)	21	19	15	55
R_e (mΩ)	46.25	43.93	35.32	
X_e (mΩ)	13.78	26.81	16.86	

A. Quasi-Static Performance Evaluation

For the first step, the SA and PSO-GA optimization algorithms are performed offline to find the minimum size of DVR and optimal tap setting of the distribution transformer. As discussed previously, this optimization algorithm considers the worst case load levels reported in Table I. In addition, the constraints are provided in Table II, and the results of optimization are given in Table III. The weighting factor, w, was considered as unity for providing a good balance between the two objectives. It is observed that the obtained optimum tap setting is -2.5% because of the high PV injection capacity. PSO-GA also resulted in a marginally better maximum V_{DVR} to be the very low value of 14.7 V. The benefit of this is the reduced voltage rating and, consequently, a lower cost and size of injection transformer (if used) and DVR system. These fixed values for tap setting of transformer and DVR size are applied to the simulation to evaluate the performance of the proposed control system.

TABLE II
Constraints of decision variable

Decision variable	**Constraints**
Tap settings T (%)	-2.5, 0, +2.5
DVR voltage V_{DVR} (V)	< 24
DVR voltage angle ϕ_{VDVR} (rad)	-π…π

TABLE III
Optimization results

Optimization Parameter	**SA**	**PSO-GA**
Tap settings (%)	-2.5	-2.5
Maximum V_{DVR} (V)	15.2	14.7
S_{DVR} = min(J) (kVA)	20.5	19.8

The quasi-static load flow analyses over a daylong period on the days of high demand and high PV generation before and after placing the DVR into the system are plotted in Fig. 5a-e. The results are shown for the load points with the highest voltage deviation from nominal voltage on each phase, which are points of 562 (phase a), 639 (phase b) and 337 (phase c) in peak demand and 562 (phase a), 899 (phase b) and 619 (phase c) in peak PV generation. The single-phase nominal voltage is 240 V, and the standard limits are about 225 V and 255 V. In the case of without DVR, the tap should be set to +2.5% to prevent under-voltages during peak demand period as shown in Fig. 5a (left). Based on this setting, however, over-voltage appears during high PV generation as seen in Fig. 5a (right). By reducing the tap setting, the over-voltage issue can be improved, but under-voltage happens during peak periods. As depicted in Fig. 5b, the DVR is able to provide enough compensation to reduce voltage deviations such that both over- and under-voltages are completely eliminated for all load points at the entire network. In addition, Table IV shows the minimum and the maximum voltage magnitudes encountered during the high demand and high PV generation periods, respectively, in the LV network with and without DVR. As observed, all voltage magnitudes are within standard limits using the proposed algorithm. In this case, both the continuous DVR compensation algorithm and the optimized tap setting work together for maintaining the voltage profile within the standard limits during high PV generation periods while preventing under-voltage during high demand periods. Thus, PVs can inject their maximum available power with no voltage violation issues. The voltage regulation has also the benefit of increased efficiency of electric motors, increased lifetime of equipment and regulated power consumption of constant impedance and constant current loads.

TABLE IV
Highest voltage deviations in the network during indicated periods.

	With DVR			**Without DVR**		
Phase	a	b	c	a	b	c
V_{min} (V) – high demand	232.5	227.5	234.2	234.5	224.7	237.4
V_{max} (V) - high PV generation	248.6	249.1	242.7	271.7	269.7	259.8

Moreover, the proposed algorithm using DVR can significantly improve the VUFD for the entire network. As observed in Fig. 5b (left and right), with DVR, VUFD considerably decreases during high demand and high generation periods compared to the case without DVR in Fig. 5a (left and right). However, as the per-phase DVR voltage in Fig. 5c (left and right) shows, at peak demand and generation, the amount of compensation, and Consequently VUFD improvement, is restricted by the DVR voltage limit. This could be improved by considering a higher weighting factor for VUFD during optimization.

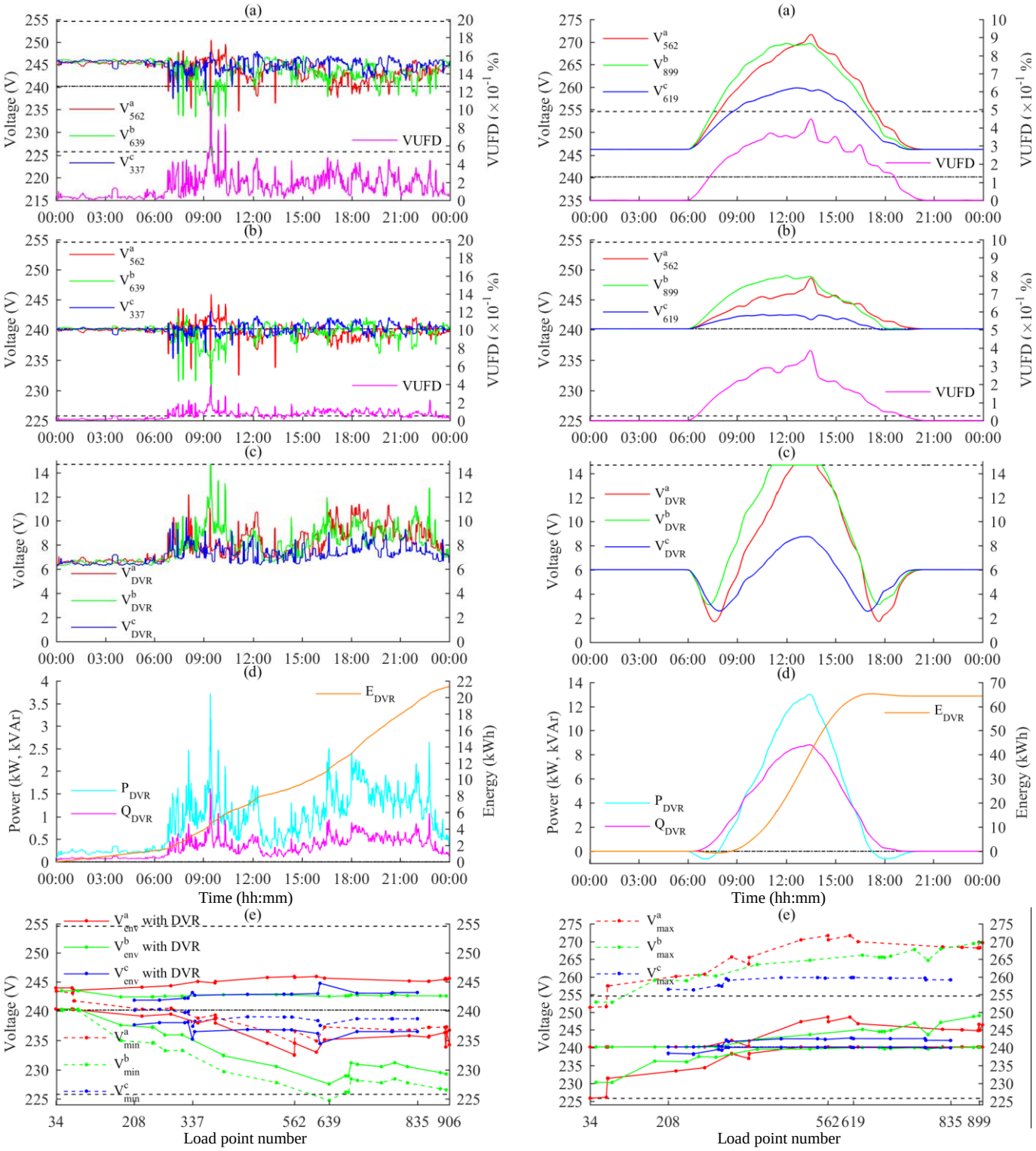

Fig. 5. High demand zero generation (left) and high generation zero demand (right) daily profiles. (a) Voltage magnitude of load points with worst peak deviation and their corresponding bus number and phase as well as VUFD without DVR; (b) same parameters with DVR in the system, (c) DVR voltage, (d) DVR output power and delivered energy, and (e) worst voltage magnitude of all load points without DVR, and the envelope of voltage magnitude variations with DVR. Standard voltage limits and DVR voltage limit are represented by dashed lines, and nominal voltage is represented by a dash-dot line.

The delivered power and energy by the 3-phase DVR, depicted in Fig. 5d, reveals that low amounts of 13 kW P and 8.8 kVAr Q peak power injections are required. As seen in Fig. 5d (right), maximum P and Q injections happen during peak PV generation period when the voltage rise is high. Moreover, during peak demand period, P and Q injections have peaked to reduce the under-voltage in the network as seen in Fig. 5d (left). The maximum utilized apparent power by the DVR is 15.7 kVA, which is just below the optimal DVR rating reported in Table III, because a small portion of the DVR capacity is spent just for phase to phase power exchange and does not appear as power injection or absorption

at the terminal of the DVR. In addition, the amount of delivered energy in the days of high PV generation and high demand profile are 64.3 kWh, and 21.3 kWh, respectively. This amount of energy and the aforementioned power can be delivered by a low rating power supply, e.g. photovoltaic source or rectifier combined with a low capacity storage unit.

It should be noted that at peak periods, the highest DVR voltage is applied, and load point voltages at the vicinity of DVR may be adversely affected by the DVR compensation. However, based on the proposed algorithm, because of the applied penalty term in the optimization objective function that puts a constraint on maximum DVR voltage, the number of voltage violations across the network is minimized. Therefore, load points in the vicinity of the DVR are not prone to voltage violations during peak periods using the proposed approach. This is illustrated in Fig. 5e that shows maximum (right) or minimum (left) voltage magnitudes of all load points without DVR as well as the envelope of voltage variations with DVR compensation. As seen in Fig. 5e (left), the voltage magnitudes of all points are within the standard limits by the DVR compensation, and the average of load point voltages is regulated towards 240 V. A similar trend can be observed in high PV generation period in Fig. 5e (right), but it causes high voltage drops at the points of 34 (phase a) and 83 (phase b). However, the proposed approach prevents voltage violations, and all load points are within the standard limits. This indicates, firstly, the ability of the control algorithm to regulate the average voltage, and secondly, that the optimization algorithm is successful in finding the appropriate ratings for DVR to minimize voltage violations.

B. Comparison with Alternative Algorithms

In order to show the advantages of the proposed algorithm, four alternative techniques are studied here including PV over-voltage protection (OVP), active power curtailment (APC), power factor control (PFC) and the combination of the two latter ones (PFC-APC). The performance of these techniques is examined in Table V by comparing the simulation results during high PV generation period.

TABLE V
Peak injected PV power and absolute Q to the upstream network by each approach in the high generation period

Algorithm	Proposed approach	OVP	APC	PFC	PFC-APC
Peak P_g (kW)	288	134	128	279	191
Peak Q_{inj} (kVAr)	3.72	1.70	1.58	195	217

The first method is OVP which trips-off PV inverter as soon as an over-voltage is detected at the grid connection point [10]. It remains off for at least 15 minutes and connects back to the network if the over-voltage condition has subsided. The performance of OVP is plotted in Fig. 6a, which shows that although voltage magnitudes are within limits, a high amount of available energy from PVs is wasted, and peak PV injection is limited to about 45% of available PV power generation.

The second alternative approach is APC presented in [13]. This method uses the droop equation in order to have a shared curtailment of injected P by PVs P_g, as a function of bus voltage V_i as given in (11).

$$P_{g,i} = P_{MPPT,i} - m\left(V_i - V_{th}^{g}\right), \quad V_i > V_{th}^{g}, P_{g,i} > 0, \tag{11}$$

where the PV inverter is controlled with the maximum power point tracking (MPPT) algorithm with the corresponding P_{MPPT}. m is the droop factor and V_{th}^{g} is the activation threshold voltage chosen to be 1.044 pu [13]. Fig. 6b shows that this approach maintains load point voltages within the standard limits. However, the high amount of curtailed power based on this technique must be stored in order not to be wasted which results in a high investment in energy storage units. Otherwise, the performance of APC is more or less comparable to OVP.

The third approach is PFC in which PV inverters inject Q as well, based on the connection point voltage level as given in (13) and (12), and to the extent that the inverter apparent power does not exceed its rating [21]. Thus, inverters work such that a distributed reactive compensation is achieved.

$$Q_{max,i} = \sqrt{S_{nom,i} - P_{g,i}}, \tag{12}$$

$$Q_{inj,i} = -Q_{max,i}\frac{V_i - V_{th}^{q}}{V_{hi}^{q} - V_{th}^{q}}, \quad V_i > V_{th}^{q}, \quad Q_{inj,i} > -Q_{max,i}, \tag{13}$$

where S_{nom} is the inverter rating, P_g is the generated power by PV, and V_{th}^{q} and V_{hi}^{q} are equal to 1.044 and 1.06 pu, respectively. The results in Fig. 6c indicate that PV injection is maximized, but due to a high amount of Q injection (negative value), which may reduce the electrical system capacity as well, over-voltage has not been eliminated. Therefore, as the last approach, PFC and APC have been used together to increase the amount of PV generation while not violating the voltage limits. In order to benefit more from Q injection, the threshold voltages of V_{th}^{q} and V_{hi}^{q} in (13) were lowered to 1.036 and 1.052 pu, respectively. The results in Fig. 6d indicate that although over-voltage is eliminated, about one-third of the available peak PV power is curtailed. The high amount of Q injection reduces the network capacity in this case as well.

As the last case in this section, the performance of PFC is compared in the high demand period. It is assumed that PV inverters have storage units or their control system can maintain the dc-link voltage. Therefore, they can inject Q during high demand periods as well. The algorithm uses modified (13) by replacing V_{hi} with V_{lo} and changing V_{th} to 0.0956. Comparing the results in Fig. 7 with Fig. 5a and Fig. 5b (left) shows that the PFC is less effective than DVR even with the higher tap setting, and it will not be able to keep voltages within the standard limits, if the tap is lowered to accommodate for the high generation profile.

Thus, the exceptional performance of the proposed algorithm in this paper using DVR compared to all the alternative methods is proved, and the available PV power injection capacity is always preserved without the need for PV power storage or high level of Q injection.

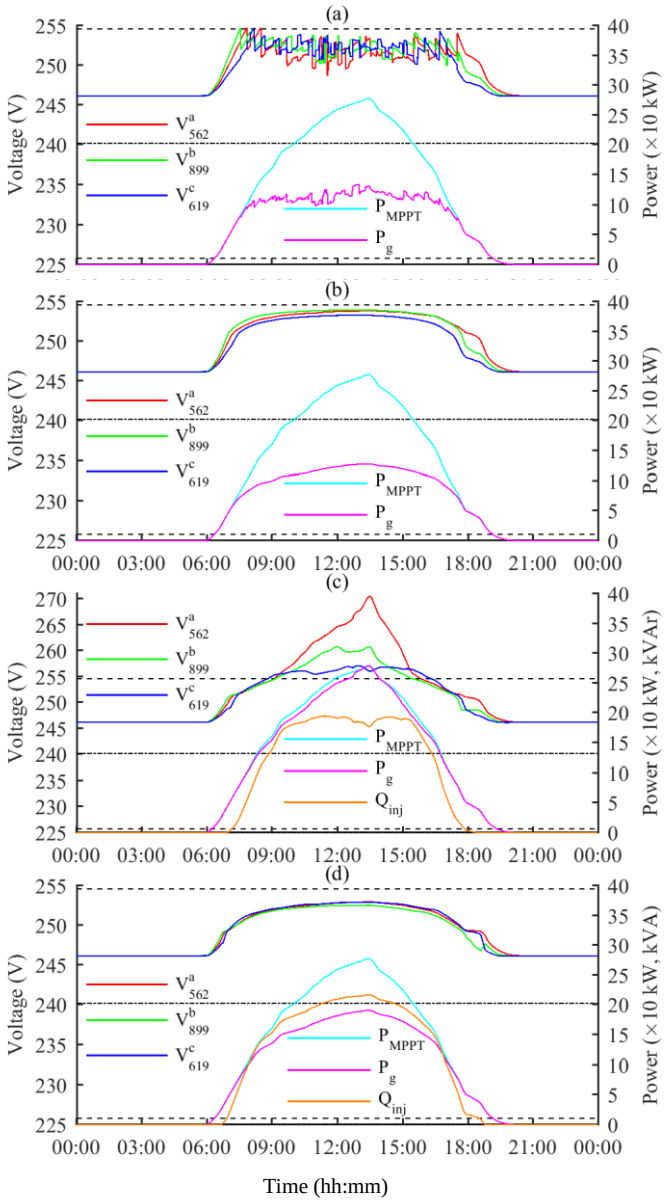

Fig. 6. High generation zero demand daily profile with (a) OVP, (b) APC, (c) PFC and (d) PFC-APC. Bus voltage magnitudes of load points with the worst voltage deviation and their corresponding bus number and phase as well as the total available PV power P_{MPPT}, total PV generation P_g and absolute total injected reactive power Q_{inj} to the upstream network at distribution transformer. Standard voltage limits are represented by dashed lines, and nominal voltage is represented by dash-dot line.

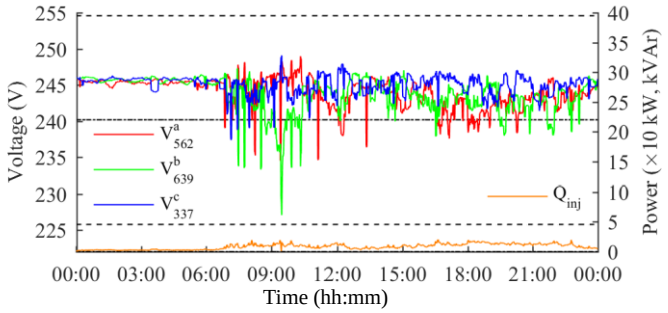

Fig. 7. High demand zero generation daily profile with PFC.

C. *Dynamic Performance Evaluation*

Simulation of system transient response to rapid variations in generation and demand, which simulates worst case sudden changes in network conditions such as sudden PV power drop, are illustrated in Fig. 8a and b. The sampling interval is equal to the grid voltage cycle of 20 ms. It is observed that the system is stable regardless of the operating point. Both the small and large step responses have also settled in about two cycles showing the high dynamic performance of the algorithm in responding to variable demand and generation profiles. Fig. 8b illustrates the voltage magnitude transient response of the worst voltage load points, observed in Fig. 5a and b. Because of the fast performance, the system is able to clear transient voltage violations in less than two grid voltage cycles. The detailed stability analysis of a grid considering distributed generations is discussed in [47].

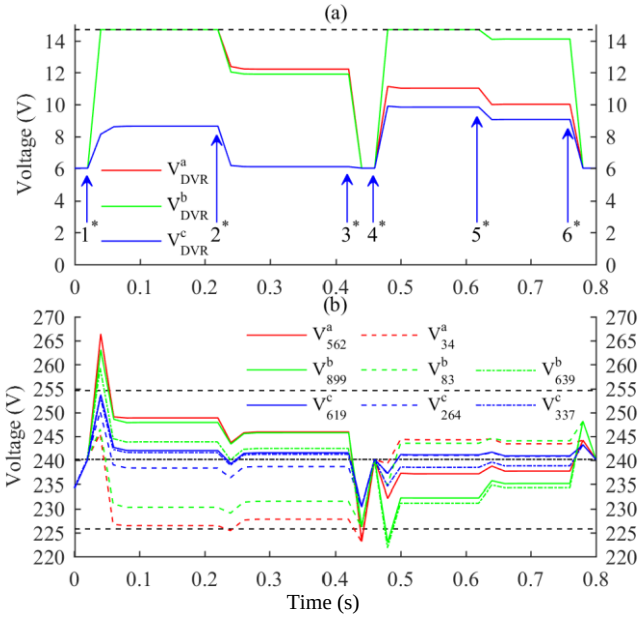

Fig. 8. Transient response of voltage magnitude of (a) DVR and (b) worst voltage load points to a step changes at all load points from zero to peak generation [1*] followed by: a small drop of 20% in generation [2*], a drop to zero generation [3*], a step change to peak demand [4*], a small drop of 20% in demand [5*], and finally, a drop to zero demand [6*]. Standard voltage limits and DVR voltage limit are represented by dashed lines.

VI. Conclusion

A continuous and real-time voltage compensation algorithm using a DVR is proposed in order to eliminate large voltage deviations in LV distribution systems. It uses an estimation of the average voltage across the network without the need for any communication links. Its performance is further improved by selecting an optimized fixed tap setting for the distribution transformer. The simulation results show that the proposed approach is able to greatly increase PV penetration in LV systems by maintaining voltage magnitude in LV system within standard limits. Comparison with alternative algorithms shows the superiority of the proposed approach in increasing PV penetration and releasing electrical system capacity with only a small amount of P and Q injection. It can also work continuously using a small storage and power source. In addition, the good dynamic response of the control system is verified considering small and large step responses. These

benefits make the proposed approach a promising solution to the voltage regulation issues in active distribution systems.

REFERENCES

[1] R. S. Committee, "Renewables 2013, Global Status Report," Renewable Energy Policy Network for the 21st Century, Paris.

[2] N.-K. C. Nair and L. Jing, "Power quality analysis for building integrated PV and micro wind turbine in New Zealand," *Energy and Buildings*, vol. 58, pp. 302-309, 2013.

[3] G. Mokhtari, G. Nourbakhsh, F. Zare, and A. Ghosh, "Overvoltage prevention in LV smart grid using customer resources coordination," *Energy and Buildings*, vol. 61, pp. 387-395, 2013.

[4] M. Bilton, N. E. Chike, M. Woolf, P. Djapic, M. Wilcox, and G. Strbac, "Impact of Low Voltage-Connected low carbon technologies on network utilisation," Imperial College London B4, 2014.

[5] B. Noone, "PV integration on Australian distribution networks," UNSW, Australia, 2013.

[6] A. Baitch. (2009). *Is it time to genuinely adopt 230 V as our distribution voltage?* Available: http://www.electricalsolutions.net.au/content/business-and-management/article/is-it-time-to-genuinely-adopt-23-v-as-our-distribution-voltage--25053451

[7] M. J. E. Alam, K. M. Muttaqi, and D. Sutanto, "An Approach for Online Assessment of Rooftop Solar PV Impacts on Low-Voltage Distribution Networks," *IEEE Transactions on Sustainable Energy*, vol. 5, pp. 663-672, 2014.

[8] R. Yan and T. K. Saha, "Voltage Variation Sensitivity Analysis for Unbalanced Distribution Networks Due to Photovoltaic Power Fluctuations," *IEEE Transactions on Power Systems*, vol. 27, pp. 1078-1089, 2012.

[9] X. Su, M. A. S. Masoum, and P. Wolfs, "Comprehensive optimal photovoltaic inverter control strategy in unbalanced three-phase four-wire low voltage distribution networks," *IET Generation, Transmission & Distribution*, vol. 8, pp. 1848-1859, 2014.

[10] "IEEE Recommended Practice for Utility Interface of Photovoltaic (PV) Systems," in *IEEE Std 929-2000*, ed, 2000.

[11] M. A. Azzouz, M. F. Shaaban, and E. F. El-Saadany, "Real-Time Optimal Voltage Regulation for Distribution Networks Incorporating High Penetration of PEVs," *IEEE Transactions on Power Systems*, vol. 30, pp. 3234-3245, 2015.

[12] R. Kabiri, D. G. Holmes, B. P. McGrath, and L. G. Meegahapola, "LV Grid Voltage Regulation Using Transformer Electronic Tap Changing, With PV Inverter Reactive Power Injection," *IEEE Journal of Emerging and Selected Topics in Power Electronics*, vol. 3, pp. 1182-1192, 2015.

[13] R. Tonkoski, L. A. C. Lopes, and T. H. M. El-Fouly, "Coordinated Active Power Curtailment of Grid Connected PV Inverters for Overvoltage Prevention," *Sustainable Energy, IEEE Transactions on*, vol. 2, pp. 139-147, 2011.

[14] J. von Appen, T. Stetz, M. Braun, and A. Schmiegel, "Local Voltage Control Strategies for PV Storage Systems in Distribution Grids," *Smart Grid, IEEE Transactions on*, vol. 5, pp. 1002-1009, 2014.

[15] G. Mokhtari, G. Nourbakhsh, G. Ledwich, and A. Ghosh, "A Supervisory Load-Leveling Approach to Improve the Voltage Profile in Distribution Network," *Sustainable Energy, IEEE Transactions on*, vol. 6, pp. 245-252, 2015.

[16] T. J. T. Hashim, A. Mohamed, and H. Shareef, "A review on voltage control methods for active distribution networks," *Przeglad Elektrotechniczny (Electrical Review). R*, vol. 88, 2012.

[17] E. Twining and D. Holmes, "Voltage compensation in weak distribution networks using multiple shunt connected voltage source inverters," in *Power Tech Conference Proceedings, 2003 IEEE Bologna*, 2003, p. 8 pp. Vol. 4.

[18] F. A. Viawan and D. Karlsson, "Coordinated voltage and reactive power control in the presence of distributed generation," in *Power and Energy Society General Meeting - Conversion and Delivery of Electrical Energy in the 21st Century, 2008 IEEE*, 2008, pp. 1-6.

[19] J. Parmar. (2011). *How reactive power is helpful to maintain a system healthy*. Available: http://electrical-engineering-portal.com/how-reactive-power-is-helpful-to-maintain-a-system-healthy/

[20] G. Mokhtari, G. Nourbakhsh, and A. Ghosh, "Smart Coordination of Energy Storage Units (ESUs) for Voltage and Loading Management in Distribution Networks," *Power Systems, IEEE Transactions on*, vol. 28, pp. 4812-4820, 2013.

[21] T. Fawzy, D. Premm, B. Bletterie, and A. Goršek, "Active contribution of PV inverters to voltage control – from a smart grid vision to full-scale implementation," *e & i Elektrotechnik und Informationstechnik*, vol. 128, pp. 110-115.

[22] G. Mokhtari, A. Ghosh, G. Nourbakhsh, and G. Ledwich, "Smart Robust Resources Control in LV Network to Deal With Voltage Rise Issue," *IEEE Transactions on Sustainable Energy*, vol. 4, pp. 1043-1050, 2013.

[23] D. Condon and D. McPhail, "Voltage regulation of distribution networks using inverter reactive power functionality - Australian utility experience," in *Power and Energy Engineering Conference (APPEEC), 2015 IEEE PES Asia-Pacific*, 2015, pp. 1-5.

[24] E. Demirok, D. Sera, R. Teodorescu, P. Rodriguez, and U. Borup, "Clustered PV inverters in LV networks: An overview of impacts and comparison of voltage control strategies," in *Electrical Power & Energy Conference (EPEC), 2009 IEEE*, 2009, pp. 1-6.

[25] S. Toma, T. Senjyu, Y. Miyazato, A. Yona, K. Tanaka, and K. Chul-Hwan, "Decentralized voltage control in distribution system using neural network," in *Power and Energy Conference, PECon 2008. IEEE 2nd International*, 2008, pp. 1557-1562.

[26] A. Ghosh and G. Ledwich, "Compensation of distribution system voltage using DVR," *Power Delivery, IEEE Transactions on*, vol. 17, pp. 1030-1036, 2002.

[27] S. Nakamura, M. Aoki, and H. Ukai, "Voltage regulation in distribution system using the combined DVR," in *International Power Electronics Conference (IPEC-Hiroshima 2014 - ECCE ASIA)*, 2014, pp. 2400-2405.

[28] S. Jothibasu and M. K. Mishra, "A Control Scheme for Storageless DVR Based on Characterization of Voltage Sags," *IEEE Transactions on Power Delivery*, vol. 29, pp. 2261-2269, 2014.

[29] G. A. d. A. Carlos, C. B. Jacobina, and E. C. d. Santos, "Investigation on Dynamic Voltage Restorers With Two DC Links and Series Converters for Three-Phase Four-Wire Systems," *IEEE Transactions on Industry Applications*, vol. 52, pp. 1608-1620, 2016.

[30] F. Jiang, C. Tu, Z. Shuai, M. Cheng, Z. Lan, and F. Xiao, "Multilevel Cascaded-Type Dynamic Voltage Restorer With Fault Current-Limiting Function," *IEEE Transactions on Power Delivery*, vol. 31, pp. 1261-1269, 2016.

[31] D. Somayajula and M. L. Crow, "An Integrated Dynamic Voltage Restorer-Ultracapacitor Design for Improving Power Quality of the Distribution Grid," *IEEE Transactions on Sustainable Energy*, vol. 6, pp. 616-624, 2015.

[32] C. Kumar and M. K. Mishra, "Predictive Voltage Control of Transformerless Dynamic Voltage Restorer," *IEEE Transactions on Industrial Electronics*, vol. 62, pp. 2693-2697, 2015.

[33] J. G. Nielsen, "Design and control of a dynamic voltage restorer," PhD, Institute of Energy Technology, Aalborg University, 2002.

[34] M. J. Reno, K. Coogan, R. Broderick, and S. Grijalva, "Reduction of distribution feeders for simplified PV impact studies," in *2013 IEEE 39th Photovoltaic Specialists Conference (PVSC)*, 2013, pp. 2337-2342.

[35] D. Santos-Martin and S. Lemon, "Simplified Modeling of Low Voltage Distribution Networks for PV Voltage Impact Studies," *IEEE Transactions on Smart Grid*, vol. 7, pp. 1924-1931, 2016.

[36] H. Sagha, "Development of innovative robust stability enhancement algorithms for distribution systems containing distributed generators," PhD, Queensland University of Technology, 2015.

[37] A. Arefi and G. Ledwich, "Maximum loadability achievement in SWER networks using optimal sizing and locating of batteries," in *2013 Australasian Universities Power Engineering Conference (AUPEC)*, 2013, pp. 1-6.

[38] A. Arefi, A. Abeygunawardana, and G. Ledwich, "A new risk-managed planning of electric distribution network incorporating customer engagement and temporary solutions," *IEEE Transactions on Sustainable Energy*, vol. 7, pp. 1646-1661, 2016.

[39] B. A. Robbins, H. Zhu, and A. D. Domínguez-García, "Optimal Tap Setting of Voltage Regulation Transformers in Unbalanced Distribution Systems," *IEEE Transactions on Power Systems*, vol. 31, pp. 256-267, 2016.

[40] P. Pillay and M. Manyage, "Definitions of Voltage Unbalance," *IEEE Power Engineering Review*, vol. 21, pp. 49-51, 2001.

[41] A. Arefi and M. R. Haghifam, "A modified particle swarm optimization for correlated phenomena," *Applied Soft Computing*, vol. 11, pp. 4640-4654, 12, 2011.

[42] J. Hromkovič, *Algorithmics for Hard Problems*, 2nd ed.: Springer-Verlag Berlin Heidelberg, 2004.

[43] T. Jen-Hao, "A direct approach for distribution system load flow solutions," *Power Delivery, IEEE Transactions on*, vol. 18, pp. 882-887, 2003.
[44] (2016). *Distribution Test Feeders*. Available: http://ewh.ieee.org/soc/pes/dsacom/testfeeders
[45] (2014). *Solar Home Electricity Data*. Available: http://www.ausgrid.com.au/Common/About-us/Corporate-information/Data-to-share/Solar-home-electricity-data.aspx
[46] S. Kumar and B. Singh, "A Multipurpose PV System Integrated to Three-Phase Distribution System Using LWDF Based Control Approach," *IEEE Transactions on Power Electronics*, vol. PP, pp. 1-1, 2017.
[47] F. Shahnia and A. Arefi, "Eigenanalysis-based small signal stability of the system of coupled sustainable microgrids," *International Journal of Electrical Power & Energy Systems*, vol. 91, pp. 42-60, 10, 2017.

Hossein Sagha received the Ph.D. degree in electrical engineering from Queensland University of Technology (QUT), Brisbane, Australia, in 2015. He is currently with EDMI Ltd Smart Energy Solutions as a Firmware Developer. His current research interests include renewable energy, power electronics, smart grid and control.

Ghassem Mokhtari received the Ph.D. degree from Queensland University of Technology (QUT) in 2014. He is now with CSIRO Australian E-Health Research Center as a Postdoc Fellow with main focus on smart home technologies and applications. He is also serving as webmaster of IEEE Queensland section and Secretary of IEEE QLD EMB chapter.

Ali Arefi (GSM'07, M'11, SM'14) received the Ph.D. degree in electrical engineering in 2011. He was a Lecturer and Research Fellow at Queensland University of Technology (QUT) from 2012 to 2015. Now, he is a Senior Lecturer at the School of Engineering and Information Technology, Murdoch University, Perth, Australia. His research interests are in the areas of electric delivery planning, state estimation, power quality, and energy efficiency.

Ghavameddin Nourbakhsh (M'13) received the Ph.D. degree from Queensland University of Technology in 2011. He joined the Queensland University of Technology, Brisbane, QLD, Australia, in 1994 as Academic Staff. His research interests include power systems operation and control, power system reliability, and cost/worth analysis.

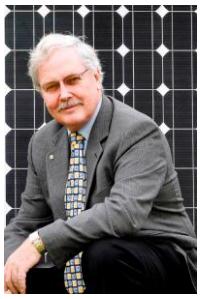

Gerard Ledwich (SM'89) received the Ph.D. degree in electrical engineering from University of Newcastle, Callaghan, NSW, Australia, in 1976. From 1997 to 1998, he was the Head of the Electrical Engineering Department, University of Newcastle. He was with the University of Queensland from 1976 to 1994. His current research interests include the areas of power systems, power electronics, and control.

Arindam Ghosh (SM'93–F'06) received the Ph.D. degree from University of Calgary, Calgary, AB, Canada, in 1983. He joined IIT Kanpur in 1985. From 2006 to 2013, he was with Queensland University of Technology, Brisbane, Australia. Currently, he is a Research Academic Professor with the Curtin University. His research interests include renewable energy and distributed generation, smart grids and power electronics applications to power systems.